VLF system for SID monitoring

Ivaylo Nachev
RCVT
Technical University of Sofia
Sofia, Bulgaria
ivaylonachev@yahoo.com

Peter Petkov
RCVT
Technical University of Sofia
Sofia, Bulgaria
pjpetkov@tu-sofia.bg

***Abstract*—This paper presents a proposal for a SID (sudden ionosphere disturbances) monitoring system based on the VLF method. The research focuses on the assembly of a solar flare monitoring system by monitoring a VLF Bafa Turkey transmitter with a working frequency of 26.7 *kHz*. The study also shows the effect of the VLF radio waves over the ionosphere. Results are presented of solar flares recorded on the territory of Sofia Bulgaria in September 2022, when multiple M-class and C-class flares were observed. The results are compared with data recorded by DIAS (Dublin Institute for Advanced Studies) as well as against data from SpaceWeatherLive and https://solarmonitor.org. There is a similarity in the results obtained from different systems, and from different geographical areas, which proves the functionality of the proposed system and the method used.**

Keywords— D-region, ionosphere, VLF, solar flare, SDR, radio astronomy, SID

I. INTRODUCTION

A solar flare is of interest for researches in the field of radio astronomy. It represents a huge explosion on the sun's surface, such explosions are usually seen near sunspots. These kinds of flares can be described as intense events and conditions with the emission of stored magnetic energy which is released in the Sun's atmosphere. A solar flare emits across the entire electromagnetic spectrum from super long wavelengths, through the microwave ranges, to the high-frequency ranges of X-rays and gamma rays [1].

Solar flares are classified as A, B, C, M, or X according to the peak flux (in general - measured in watts per square meter, W/m2). Each X-ray class category is divided on a logarithmic scale from 1 to 9, e.g. B1 to B9, C1 to C9, etc. An X2 flare is twice as powerful as an X1 type flare and is four times more powerful than an M5 flare. The category of X-class eruptions is slightly different and does not stop until X9 but continues. Solar flares of X10 or stronger are also sometimes called Super X-class solar flares [2,3].

A solar flare leads to a sudden increase in extreme ultraviolet (EUV) and X-ray radiation on Earth affecting the ionosphere diurnal layers. When a solar eruption occurs charged photons from it penetrate to the ionosphere D-layer (~60-90 *km* altitude) increasing its ionization and electron density. This type of solar activity leads to significant interference in the received amplitudes of very low-frequency radio signals (VLF band) at a frequency range between 3 and 30 *kHz*. Their propagation is through an effect resembling a waveguide due to the propagation of waves between the ground and the ionosphere [4]. According to the magnitude of the solar flare reaching the earth, the D - a layer of the ionosphere is affected differently, which in turn causes a disturbance in the VLF radio signals (characterized by up to a few dB change in signal level), therefore this disturbance can be used to monitor solar activity [5].

Solar flare's effects on the D-layer are also found in the literature as sudden ionospheric disturbances (SID). SID is any one of several ionospheric disturbances resulting from unusually high ionization/plasma density in the D region of the ionosphere and caused by a solar flare. SID results in a sudden increase in radio wave absorption that is most severe in the VHF, UHF, HF, and VFL frequency bands and, as a result, often disrupts or interferes with telecommunications systems. Attenuations are characterized by sudden onset and recovery that takes minutes or hours [5].

The ionospheric disturbance causes a change in the VLF wave signal level. Scientists can use this enhancement to detect solar flares; by monitoring the signal strength of a remote VLF transmitter, sudden ionospheric disturbances (SIDs) are recorded and indicate when solar flares have occurred. The small geomagnetic effect in the lower ionosphere appears as a small hook on the magnetic records and is therefore called the "geomagnetic crochet effect" or "sudden field effect"[5, 6].

The research presented a low-cost and reliable solar flare monitoring system verified for work by monitoring the amplitude variation of a radio signal ($f_o = 26.7kHz$) from a Bafa Turkey VLF transmitter (37° 30′ N 27° 25′ E). The design and setup of the system's sensor, a loop antenna, is discussed in detail, in contrast to other studies in the field where different types of audio cards are used as the receiving device, the possibility of using different types of software-defined radio(SDR) and a spectrum analyzer is also discussed here. The data obtained from the solar activity survey for the period between September 2022 on the territory of Sofia, Bulgaria are compared with data recorded by DIAS (Dublin Institute for Advanced Studies). Data presented by SpaceWeatherLive - a Belgian non-profit organization presenting information combined information from several sources in the field of

979-8-3503-9834-2/23/$31.00 ©2023 IEEE

astronomy, space weather, aurora, and other topics in the field including solar flare tracking, as well as data from https://solarmonitor.org/index.php.

II. Loop Antenna Design And Setup

The designed system (figure 1) was installed in the area of Sofia, Bulgaria (42°32'47.4 "N 23°22'23.5 "E), and monitoring signals from a 26.7 kHz signal from a Bafa Turkey VLF transmitter (37° 24'43 "N 27°19'25 "E). The system consists of a loop antenna, an amplifier, a software-defined radio (several options for the device receiving the antenna data have been considered), and a computer with the appropriate software to process and record the data.

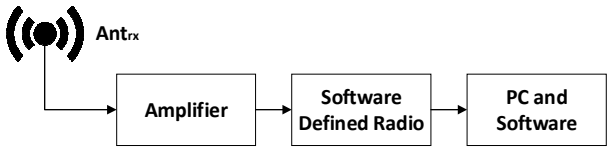

Fig.1. Designed system block diagram.

The loop antenna must be designed for a transmitter frequency $f_o = 26.7kHz$. A construction (resembling a square with 60 cm sides) allowing 140 turns of copper wire with a diameter of 0.4 mm is used. However, the loop antenna thus constructed has the following characteristics: $R_L = 31.2\,\Omega$, $Q = 530$, $f_r = 31kHz$. To make the antenna resonate at 26.7 kHz it is necessary to tune it by the method of tuning a parallel RLC circuit by adding a parallel coupled capacitance to the antenna - Fig. 2. In this case to obtain a resonant frequency $f_r = 26.7kHz$ the added capacitance $C = 570pF$.

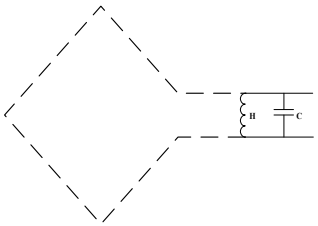

Fig.2 a). Loop antenna resonant circuit - block diagram.

Fig.2 b). Loop antenna – real life model.

The antenna frequency response is presented in the figure 4. The measured frequency response of the antenna is taken for the range from 18 to 30 kHz and it is seen that the resonance is at 26.7 kHz. For this purpose, an oscillator (pos. (4), refer Fig. 3 b) is used for the transmitting side to which a high-frequency coil (3) from a loudspeaker with an approximate resonant frequency of 30 kHz is connected. On the receiving side, the designed sensor (2) is connected to an oscilloscope (1) (instead of using an oscilloscope, it is possible to use a spectrum analyzer), used to measure the amplitude of the transmitted signal. Due to the non-differential input of the oscilloscope and the output of the generator and the differential inputs of the speaker coil and the designed antenna, they are connected through a 1:1 transformer to the respective measuring instruments. The used experimental setup for loop antenna tuning is presented in Figure 3 b). An amplifier with gain $Gamp17.2dB$ was used to increase the sensitivity of the system.

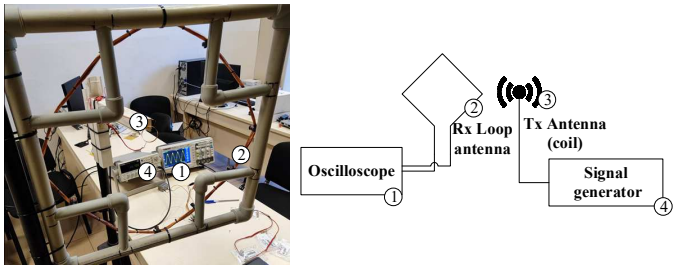

Fig.3 The calibration setup. a) the experimental setup, b) block diagram of the setup.

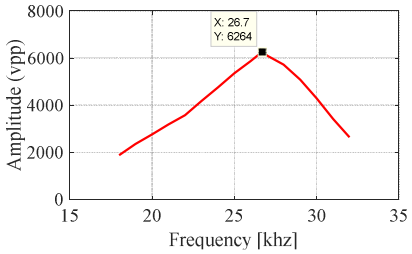

Fig.4 Loop antenna frequency response.

III. Analysis Of The Obtained Results

The VLF band is used for several radio navigation services (systems working on the principle of the OMEGA system, used to determine the exact location of ships and aircraft by triangulation using low-frequency signals in the range between 15 and 30 kHz), government radio systems for precise timing (transmitting signals for synchronization and setting radio clocks)[7]. VLF signals find great application in military communication, due to the nature of radio waves in this range, they can pass a range of over 40 meters in underwater communication in salt water, making them suitable for use in submarine communication. The VLF technologies listed use transmitters emitting a continuous signal over time with equal amplitude. When solar activity changes the ionosphere, these signals change their level by a few decibels. This change is most evident when day and night change and vice versa (grey line, day-night). Since the ionospheric disturbances caused by solar flares result in signal fluctuations of a few decibels, the tracking of these signals can be used to track solar flares [8, 9].

The conductivity of the layers composing the D-layer has the property of electrical conductivity in the "upper wall of the waveguide"(waveguide earth - ionosphere) in the path of the electromagnetic wave of the VLF signal and therefore leads to a change in all their propagation parameters. These changes are detected in the form of field strength variation of the VLF. Although the effects on the VLF signal are always well

recognizable, they can be complex to analyze for specific radio paths. The theory of VLF propagation through the ground-ionosphere waveguide under regular (quiet) ionospheric conditions is well established [10]. The sudden onset of solar activity shows the most pronounced change in the VLF signal parameters, characterized by a jump in amplitude, followed by its gradual recovery within a small time interval (usually within about an hour), which corresponds to the duration of atypical solar activity/duration of solar flare [11, 12].

Although the locations in the ionosphere "attacked" by solar flares do not always coincide with the path of the VLF radio wave path, reliable results have been observed in monitoring this type of solar activity by monitoring the low-frequency signal through stations very similar to the described type. In the present study, however, the Bafa Turkey transmitter broadcasting a signal at 26.7 *kHz* was chosen, whose radio path direction coincides with the coordinates at which the study was conducted. For the period from 10 September 2022 to 20 September 2022, more than 10 eruptions were recorded, among which M-class eruptions were observed. A system whose block diagram is shown in Figure 1 was used. An SDR type RSP1 Msi2500 Msi001 with an active VLF antenna and a Signal hound spectrum analyzer sa44b were used as the SDR device. Figure 5 present data from 17 September 2022, when there were significant sustained M 2.6 class solar flares, with even smaller C class flares being detected. The obtained results from a SDR type RSP1 Msi2500 Msi001 with an active VLF antenna and using the SDRConsole (V3) software are completely incomprehensible. It is possible that the RSP1 is sensitive to the power mains hum from the pulse power supply of the antenna, having a wide bandwidth. Further investigation of this type of SDR with a designed loop antenna is needed to see if this device would be functional for VLF monitoring.

Obtained results in Fig. 5 are compared with results from DIAS - Fig.6, results recorded from https://solarmonitor.org/index.php - Fig. 7, and SpaceWeather Live data - Fig. 8, which shows that the periods of detected activity match the indicated sources used for comparison.

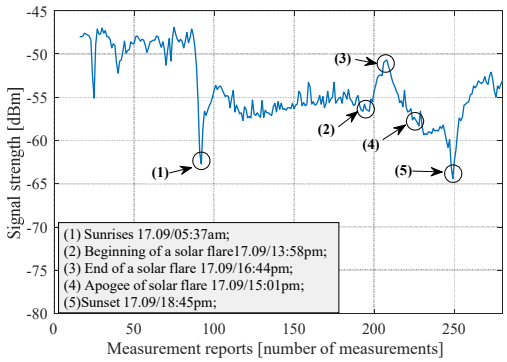

Fig.5. Detected solar flares on 17/09/2022 obtained by the proposed system and Signal Hound spectrum analyzer sa44b.

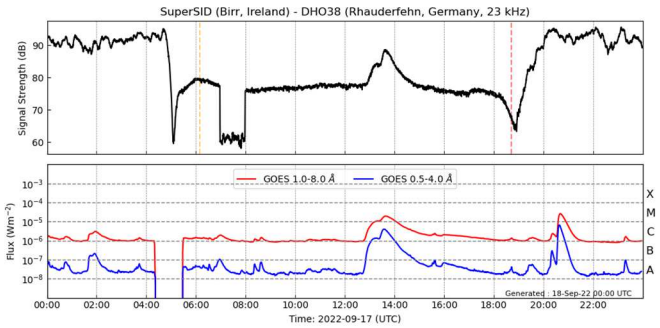

Fig. 6. Data of the activity of solar flares for 17/09/2022. recorded by the Dublin Institute for Advanced Studies.

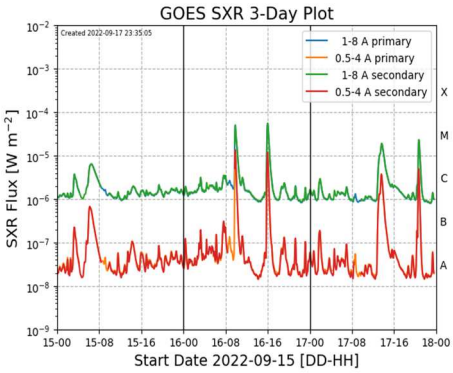

Fig. 7. Data of the activity of solar flares for 17/09/2022. recorded by https://solarmonitor.org/index.php.

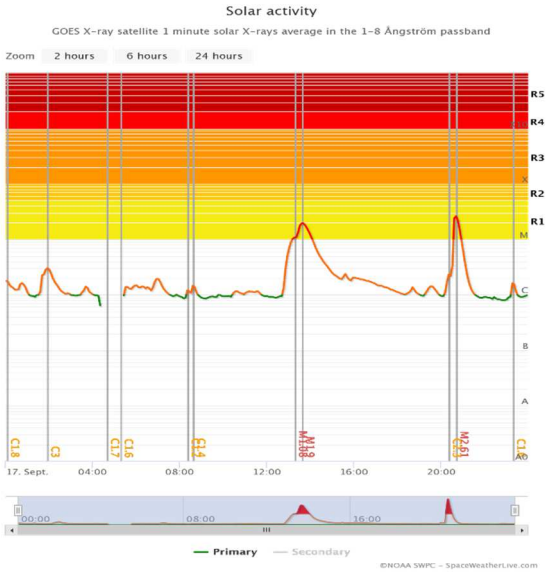

Fig. 8. Data of the activity of solar flares for 17/09/2022 recorded by SpaceWeatherLive.

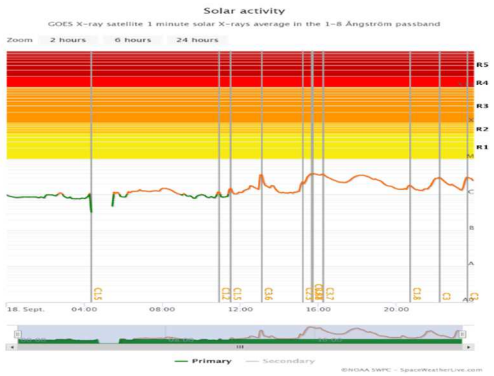

Fig. 9. SpaceWeatherLive solar flares data for 18/09/2022 recorded by SpaceWeatherLive.

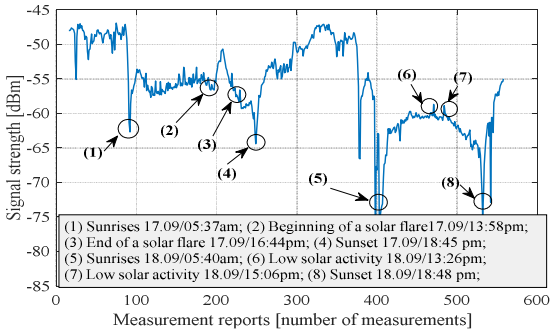

Fig.10. Detected solar flares on 17-18 September 2022 obtained by the proposed system and Signal Hound sa44b

From the presented figures 6 - 10, it can be seen that the data obtained by the considered system are similar to the data used for comparison by already existing solar flare tracking systems. The system is suitable for detecting solar flares of class M and weak flares of class C.

Similar system was presented in [13] based of Cambridge superSID platform. Development [13] despite its good sensitivity imposes a limitation on the use of hardware (refer to fig. 1) and used software to analyze the obtained results. That limits the possibility to improve and optimize the system, compared to the system proposed in this paper, where each element can be optimized.

IV. Conclusion

The proposed system for monitoring ionospheric disturbances in the D layer caused by solar flares by monitoring VLF signals shows good results. The results were obtained by monitoring the solar activity on the territory of Sofia, Bulgaria, showing that such a system is fully functional for long-term monitoring of this type of solar activity. The refinement of this type of system enables the classification of different class solar flares by their effect on the lower ionosphere layers, as well as further research in the field of electromagnetic propagation showing the possible mechanisms of VLF propagation in disturbed conditions. The project's future includes expanding the system's operating frequency range, by using several antennas for monitoring different VLF transmitters signals, and developing and selecting of suitable amplifier and multiplexer.

The obtained results are reliable and, unlike conventional methods in the scientific field where the emphasis is placed on the study of ionization from solar flares, their effects on radio signals are observed directly. The system is easy to multiply, and synchronization between separate mounted base stations at distant geographic coordinates would give detailed information on solar activity and VLF signal propagation over them.

Acknowledgment

The paper is supported by Horizon 2020 TWINNINGS program, project STELLAR, grant ID: 952439.

References

[1] S. M. Hamdi, D. Kempton, R. Ma, S. F. Boubrahimi, and R. A. Angryk, "A time series classification-based approach for solar flare prediction," 2017 IEEE International Conference on Big Data (Big Data), Boston, MA, USA, 2017, pp. 2543-2551, doi: 10.1109/BigData.2017.8258213.

[2] D. P. Grubor, D. M. Šulić, and V. Žigman, "Classification of X-ray solar flares regarding their effects on the lower ionosphere electron density profile," Ann. Geophys., vol. 26, no. 7, pp. 1731–1740, 2008, doi: 10.5194/angeo-26-1731-2008.

[3] P. Velinov, "Major X-class solar flare from Earth-facing active region AR12887 on October 28, 2021 and first cosmic ray GLE 73 in solar cycle 25," C. R. Acad. Bulgare Sci., vol. 75, no. 2, pp. 248–258, 2022, doi: 10.7546/CRABS.2022.02.10.

[4] S. Guyer and Z. Can, "Solar flare effects on the ionosphere," 2013 6th International Conference on Recent Advances in Space Technologies (RAST), Istanbul, Turkey, 2013, pp. 729-733, doi: 10.1109/RAST.2013.6581305.

[5] W. Xu et al., "VLF Measurements and Modeling of the D-Region Response to the 2017 Total Solar Eclipse," in IEEE Transactions on Geoscience and Remote Sensing, vol. 57, no. 10, pp. 7613-7622, Oct. 2019, doi: 10.1109/TGRS.2019.2914920.

[6] G. Chen et al., "Multi-Instrument Observations of the Atmospheric and Ionospheric Response to the 2013 Sudden Stratospheric Warming Over Eastern Asia Region," in IEEE Transactions on Geoscience and Remote Sensing, vol. 58, no. 2, pp. 1232-1243, Feb. 2020, doi: 10.1109/TGRS.2019.2944677.

[7] R. A. Marshall, T. Wallace, and M. Turbe, "Finite-Difference Modeling of Very-Low-Frequency Propagation in the Earth-Ionosphere Waveguide," in IEEE Transactions on Antennas and Propagation, vol. 65, no. 12, pp. 7185-7197, Dec. 2017, doi: 10.1109/TAP.2017.2758392.

[8] H. Lu et al., "ELF/VLF Communication Experiment by Modulated Heating of Ionospheric Auroral Electrojet at EISCAT," in IEEE Transactions on Antennas and Propagation, vol. 69, no. 4, pp. 2267-2273, April 2021, doi: 10.1109/TAP.2020.3026872.

[9] S. A. Cummer, "Modeling electromagnetic propagation in the Earth-ionosphere waveguide," in IEEE Transactions on Antennas and Propagation, vol. 48, no. 9, pp. 1420-1429, Sept. 2000, doi: 10.1109/8.898776.

[10] J. R. Wait, "Reflection of VLF radio waves at a junction in the Earth-ionosphere waveguide," in IEEE Transactions on Electromagnetic Compatibility, vol. 34, no. 1, pp. 4-8, Feb. 1992, doi: 10.1109/15.121660.

[11] A. Kolarski and D. Grubor, "Comparative analysis of VLF signal variation along trajectory induced by X-ray solar flares," J. Astrophys. Astron., vol. 36, no. 4, 2015, doi: 10.1007/s12036-015-9361-x.

[12] J.-P. Raulin et al., "Solar flare detection sensitivity using the South America VLF Network (SAVNET): SOLAR FLARE DETECTION," J. Geophys. Res., vol. 115, no. A7, 2010.

[13] W. P. Wah, M. Abdullah, A. M. Hasbi, and S. A. Bahari, "Development of a VLF receiver system for Sudden Ionospheric Disturbances (SID) detection," 2012 IEEE Asia-Pacific Conference on Applied Electromagnetics (APACE), Melaka, Malaysia, 2012, pp. 98-103, doi: 10.1109/APACE.2012.6457640.